Available online at www.sciencedirect.com

ScienceDirect

Procedia Structural Integrity 2 (2016) 986–993

Structural Integrity Procedia

www.elsevier.com/locate/procedia

21st European Conference on Fracture, ECF21, 20-24 June 2016, Catania, Italy

# Effects of strain rate on mechanical properties in tension of a commercial aluminium alloy used in armour applications

Ezio Cadoni[a,*], Matteo Dotta[a], Daniele Forni[a], Hanspeter Kaufmann[b]

[a] *University of Applied Sciences of Southern Switzerland, Campus SUPSI Trevano, Canobbio 6952, Switzerland*
[b] *RUAG Defence AG, Thun 3602, Switzerland*

**Abstract**

The use of aluminium alloys in the construction of defense vehicles is strongly increasing in these last decades because they require new lightweight armours for improving their survivability without sacrificing efficiency and performance. In this paper the effects of strain rate on the mechanical properties in tension of a commercial aluminium alloy AA7081 is analyzed. The tests have been carried out by means of three different set-ups for quasi-statics, medium and high strain rates. For the high and medium strain rate tests have been used respectively a Split Hopkinson Tension Bar device and a Hydro-pneumatic machine installed in the DynaMat Laboratory of the University of Applied Sciences of Southern Switzerland-Lugano. The results show: an increase of the stress at a given strain when increasing the strain-rate from $10^{-3}$ to $10^{3}$ $s^{-1}$, a strain-rate sensitivity of the uniform and fracture strain, a moderate reduction of the cross-sectional area at fracture with increasing the strain-rate. Based on these experimental results the parameters required by the Johnson-Cook constitutive law have been determined.


Peer-review under responsibility of the Scientific Committee of ECF21.

*Keywords:* High strain-rate; Aluminium alloy; Split Hopkinson Tensile Bar; Hydro-Pneumatic Machine.

## 1. Introduction

Aluminium alloys are attractive engineering materials for many applications, such as chemical, aerospace industries, aeronautical and automotive. Light armored vehicles are an example of this application. The requirement in the construction of defense vehicles of new lightweight armours for improving their survivability without sacrificing efficiency and performance, lead to a strong increase in the use of aluminium alloys. Composition, strain-rate, microstructure and temperature influence on the mechanical properties and failure mechanism of aluminium alloys were investigated for example by Higashi et al. (1991) and Peixinho and Doellinger (2010). Singh et al. (2012, 2013), studied the dynamic compressive and tensile behavior of the aluminium alloy, AA6063-T6 in the strain rate range from 0.001 $s^{-1}$ to 850 $s^{-1}$. Tanimura et al. (2009) studied the dynamic behavior of several classes of aluminium alloys by means of sensing block type high speed material testing system. Oosterkamp et al. (2000) analyzed the strain rate sensitivity of two commercial aluminium alloys AA6082 and AA7108 in peak temper T6 and overaged T79 in

* Corresponding author. Tel.: +41-58-666-6377 ; fax: +41-58-666-6359.
*E-mail address:* ezio.cadoni@supsi.ch


Peer review under responsibility of the Scientific Committee of ECF21.
10.1016/j.prostr.2016.06.126

compression and in a wide range of strain rates, from 0.1 to 3000 $s^{-1}$ at room and high temperature (around 500°C) observing a trend of negative strain rate sensitivity for strain rates greater than 2000 $s^{-1}$, as a consequence of the strain localization on a microscopic scale. Chen et al. (2009) did an experimental campaign addressed to study the stress-strain behavior of extruded aluminium alloys AA6060, AA6082, AA7003 and AA7108 in T6 temper in a wide range of strain rates. Tensile tests at high rates of strain were carried out by using a Split Hopkinson Tension Bar apparatus. They highlighted how the AA6060-T6 and AA6082-T6 exhibited only slight sensitivity to the strain rate, as a consequence these alloys could be modeled as rate-insensitive with good accuracy. Differently for the AA7003-T6 and AA7108-T6 alloys where a marked sensitivity to strain rate was revealed and consequently included in simulations. Finally, Cadoni et al. (2012a) analyzed two aluminium alloys used in defense vehicles showing negative strain rate sensitivity for the AA5059-H131 alloy and positive for the AA7039-T651 alloy.
Thus, the first objective of this work is the examination of the strain-rate sensitivity in a wide range of strain-rate on the mechanical properties in tension of the AA7081 commercial aluminium alloy. Secondly, the experimental data are used to obtain the parameters of the Johnson-Cook constitutive material relationship.

### *1.1. Material*

The analysed material is part of the 7xxx series zinc (Zn) based aluminium alloy, AA 7081. This alloy has an high yield and tensile strengths and provide increased ballistic protection. The chemical composition is shown in Table 1.

Table 1. Chemical composition of Aluminium Alloy 7081.

| Constituents | Si | Fe | Cu | Mn | Mg | Zn | Cr | Ti | Al |
|---|---|---|---|---|---|---|---|---|---|
| wt.% | 0.02 | 0.05 | 1.51 | <0.01 | 1.80 | 7.28 | <0.01 | 0.04 | 89.20 |

### *1.2. Specimen*

Round samples having 3mm in diameter and 5mm of gauge length have been used. In order to measure the fracture parameters on the specimens surface, the gauge length of 5 mm has been marked before the test see more details in Cadoni et al. (2011b, 2013, 2014). The specimens analysis has been carried out studying both the experimental results in terms of engineering and true stress versus strain curves and in terms of fracture failure. The characteristics of fracture as the reduced area of the specimen cross section after failure in the necking zone as well as the fracture strain have been obtained by means of two images taken before and after the test of each specimen. In order to do this, the specimen is at best reconstructed by bringing together the two broken parts, so that both the diameter and the meridional radius of curvature at the reduced section could be measured.

## 2. Experimental Setup

### *2.1. The testing procedure*

The mechanical properties of AA7081 are studied by three different experimental techniques. The quasi-static tests are conducted on electromechanical universal testing machine, which has the maximum load bearing capacity of 50 kN. Medium and high strain rate experiments have been performed on hydro-pneumatic machine and Split Hopkinson Tensile Bar apparatus respectively, whose working principles are described in the following sections.

### *2.2. Hydro-Pneumatic Machine (HPM)*

The medium strain rate tests have been carried out on a Hydro-Pneumatic Machine (HPM) (Cadoni et al. (2012a)) as shown in Fig.1. This HPM has a cylindrical tank, which is divided into two chambers by a sealed piston. At the beginning of the test one chamber, which is nearer to the specimen, is filled with gas (generally air) at high pressure

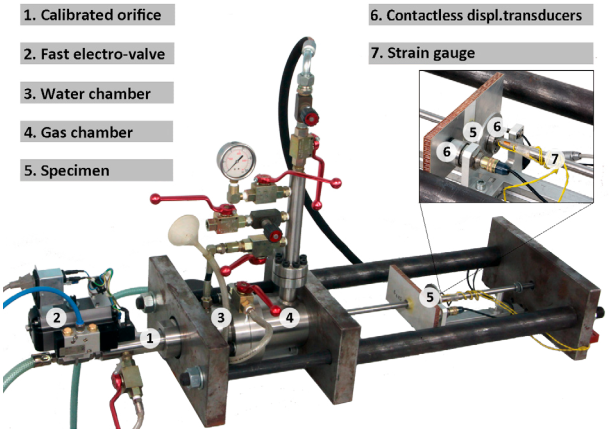


Fig. 1. Hydro-Pneumatic Machine for intermediate strain rate tests.

(e.g. 150 bars) and the other one is filled with water. Equal pressure is established in both the chambers so that the forces acting on the two piston faces are in equilibrium. The end of the piston shaft is connected to one end of the specimen and another end of the specimen is connected with an elastic bar, which is rigidly fixed to the machine. This elastic bar is instrumented with a strain gauge whose function is to measure the load resisted by the specimen during the test. The way the test is performed has been extensively reported in Cadoni et al. (2012b, 2011a); Asprone et al. (2009).

### *2.3. Split Hopkinson Tensile Bar (SHTB) apparatus*

The Split Hopkinson Tensile Bar apparatus is shown in Figure 2, additional information can be found in Albertini and Montagnani (1976, 1984); Cadoni et al. (2012b, 2013). In this set up, the pretensioned bar (2) is the continuation of the input bar (4) and thus the difficulties connected to the launching and impacting of projectiles as created in traditional split Hopkinson pressure bar (SHPB) are avoided. The SHTB apparatus is installed in the DynaMat Laboratory of the University of Applied Sciences of Southern Switzerland. It is composed by two cylindrical high strength steel bars, having a diameter of 10 mm with a length of 9 m and 6 m for input bar (combined with pretensioned bar) and output bar (7), respectively. The round specimen (6) is screwed to the two bars as shown in Figure 2. The material of the bars is C85S steel, which has modulus of elasticity, $E = 193$ GPa and density, $\rho = 7908$ kg/m$^3$. Therefore, the wave speed in the bar is $C = \sqrt{E/\rho} = 4938$ m/s.

This configuration of SHTB can generate very long loading pulses and such long duration loading pulses are required for testing very ductile materials, Cadoni et al. (2011a). A tensile mechanical pulse of 2.4 ms duration with linear loading rate during the rise time (30 $\mu$s) is generated under tensile loading.

On the input and output bars are glued two semiconductor strain gauges which measure the incident, reflected and transmitted pulses acting on the cross section of the specimen. The test with the MHB is performed as follows: i) first a hydraulic actuator (1), of maximum loading capacity of 600 kN, is pulling part of the input bar (6m) as pretension bar with a diameter of 10 mm; the pretension stored in this bar is resisted by the blocking device (3); ii) second operation is the rupture of the brittle bolt in the blocking device which gives rise to a tensile mechanical pulse of 2.4 ms duration with linear loading rate during the rise time, propagating along the input and output bars bringing to fracture the specimen. The semi-conductor strain-gage station (5) is glued on the input bar at 750 mm from the specimen with the aim of to record the deformation $\epsilon_I(t)$ of the bar caused by the incident tension pulse during the propagation toward the specimen and the deformation $\epsilon_R(t)$ caused by the part of the incident tension pulse reflected at the interface incident bar-specimen, reflection which is correlated with the deformation of the specimen; the distance of the strain-gage station from the specimen is chosen in a way to distinguish clearly the record of the incident pulse from the record of the reflected pulse. A second semi-conductor strain-gauge station is glued on the output bar (8) at the same distance from the specimen as the strain-gauge station on the incident bar; this second strain-gauge station is used to record the deformation $\epsilon_T(t)$ caused on the bar by the part of the incident pulse which has been sustained

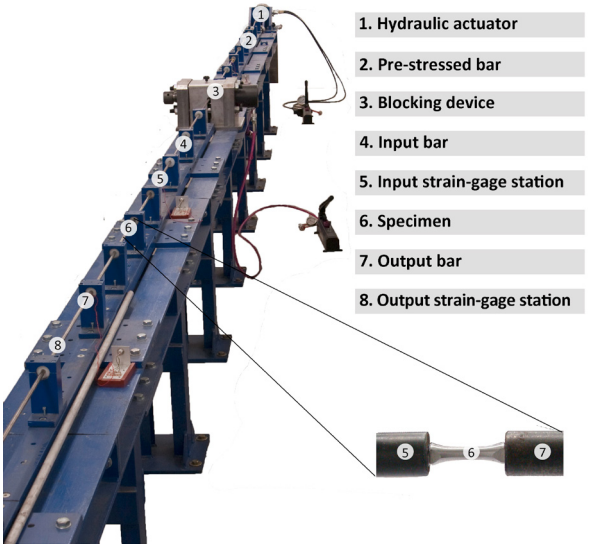


Fig. 2. Split Hopkinson Tensile Bar

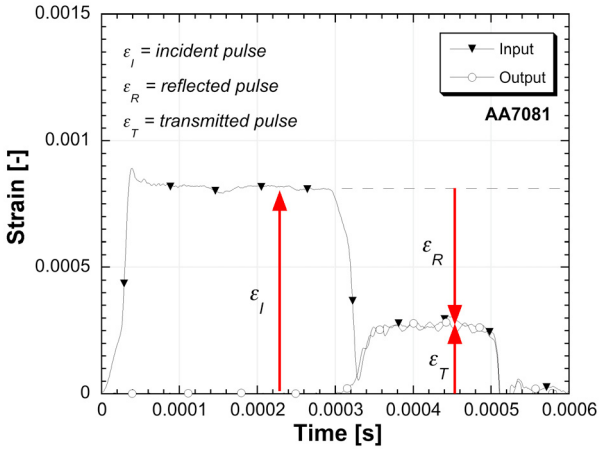


Fig. 3. Raw signals obtained in a tensile test by using the Split Hopkinson Tensile Bar

by the specimen and has been therefore transmitted in the output bar. One non-filtered record of a dynamic tension test on high strength specimen performed with the SHTB is shown in Fig. 3 where it possible to observe: the clean resolution of incident, reflected and transmitted pulses; the sharp rise time of the incident pulse of the order of 30 $\mu$s; the nearby constant amplitude of the incident pulse; the characteristic similitude of the record of the transmitted pulse with the stress-time record of a conventional tension test.

On the basis of the record of $\epsilon_R(t)$ and $\epsilon_T(t)$ of Fig. 3, of the consideration of the basic constitutive equation of the input and output elastic bar material, of the one-dimensional wave propagation theory it is possible to calculate the engineering stress ($\sigma_s$), engineering strain ($\epsilon_s$ ) and strain rate ($\dot{\epsilon}_s$) by the following equations (Albertini and Montagnani (1976); Riganti and Cadoni (2014)):

$$\sigma_s(t) = E_0 \cdot \frac{A_0}{A}\epsilon_T(t) \tag{1}$$

$$\epsilon_s(t) = -\frac{2 \cdot C_0}{L}\int_0^t \epsilon_R(t) \tag{2}$$

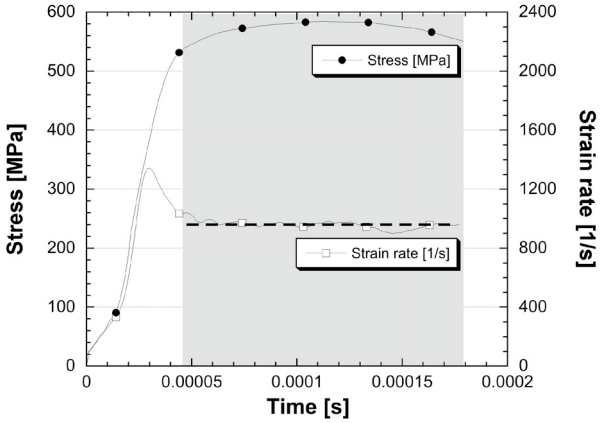


Fig. 4. Stress and strain rate versus time curves

$$\dot{\epsilon}_s(t) = -\frac{2 \cdot C_0}{L}\epsilon_R(t) \tag{3}$$

where, $E_0$ is the Young's modulus of elasticity for the bar material, $A_0$ is the cross-sectional area of the bar, $A$ is the cross-sectional area of the specimen and $L$ is the gauge length of the specimen.

## 3. Results

The mechanical response in tension and in a wide range of strain-rates of the aluminium alloy 7081 showed a positive strain-rate sensitivity at medium and high strain-rates respectively. A moderate strain-rate sensitivity of uniform and fracture strain was observed. Finally, increasing the strain-rate, also a reduction of sectional area was achieved. Figure 5 and Table 2 presents the results, in terms of representative engineering and true stress versus strain curves, of the quasi-static and dynamic mechanical tests at the three strain-rates selected. A good repeatability of tests at different strain-rates was noted.

Table 2. Experimental results.

| Strain rate [$s^{-1}$] | Yield stress [MPa] | UTS [MPa] | Uniform strain [%] | Fracture strain [%] | True tensile stress [MPa] | True uniform strain [%] | Reduction of area [%] |
|---|---|---|---|---|---|---|---|
| 1000 | 534±27 | 588±3 | 8.2±0.7 | 15.6±1.3 | 635±5 | 7.8±0.7 | 28.7±2.3 |
| 300 | 550±7 | 586±7 | 7.7±0.1 | 17.8±1.9 | 631±7 | 7.4±0.1 | 30.4±3.0 |
| 30 | 541±10 | 580±6 | 6.7±1.3 | 13.9±1.1 | 619±15 | 6.4±1.27 | 31.6±1.5 |
| 0.001 | 529 | 563 | 4.8 | 14.1 | 590 | 4.7 | 42 |

A better and brief representation of the strain-rate sensitivity of this alloy can be obtained by examining the trends of the yield strength and the ultimate tensile strength (at the onset of necking) as a function of strain-rate (Fig. 6). In the same plots also the uniform and fracture strain and the reduction in cross-sectional area are reported. For each of these trends, a visual trend line is included to help distinguish the data sets. Finally, post-mortem examination of specimens has also been made after fracture by measuring the diameter and the meridional radius of curvature at the reduced section as shown in Fig. 7a. These data are used for the evaluation of the last point of the true stress-strain diagram (see Fig. 7b) by the Bridgman (1952) formulae.

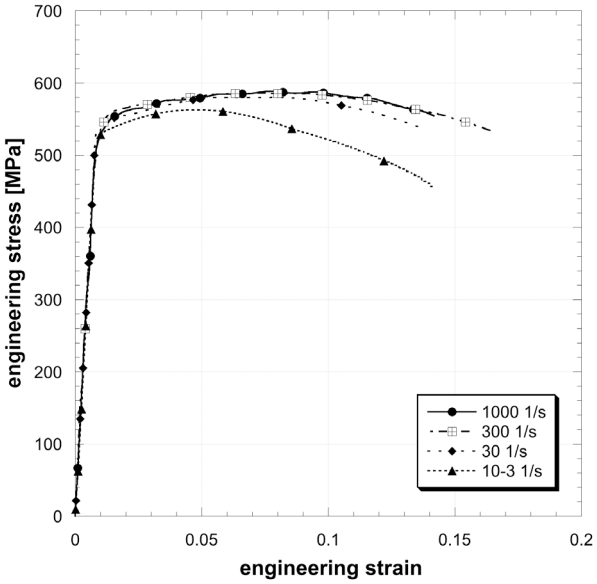


Fig. 5. Stress versus strain curves obtained at different strain rates.

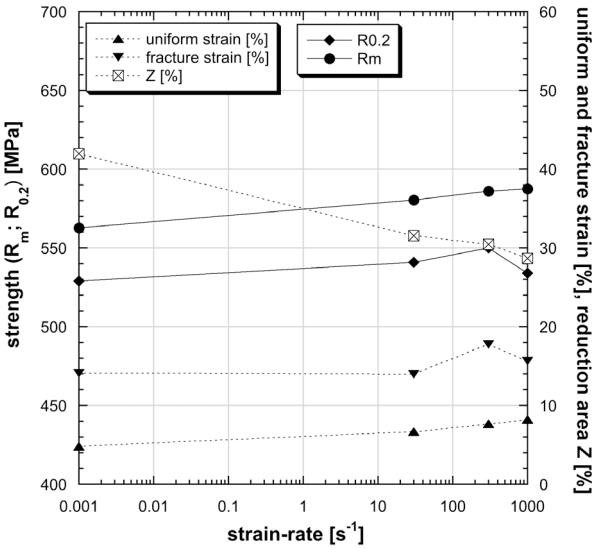


Fig. 6. Strain rate sensitivity.

## 4. Material constitutive relationship

A well known and extensively used strength model for predicting the behaviour of elastoplastic materials including isotropic hardening and strain rate hardening is the the Johnson-Cook material model (see Johnson and Cook (1985)), that can be expressed as:

$$\sigma_{JC} = \left(A + B \cdot \epsilon_p^n\right) \cdot \left(1 + C \cdot ln(\dot{\epsilon}^*)\right) \tag{4}$$

where, $\epsilon_p$ is the equivalent plastic strain, $\dot{\epsilon}^* = \dot{\epsilon}/\dot{\epsilon}_0$ is the dimensionless plastic strain rate for $\dot{\epsilon}_0 = 0.001\,\mathrm{s}^{-1}$ and the considered strain rate $\dot{\epsilon}$. The constants $A$, $B$, $C$ and $n$ are the four material parameters, which are determined by using

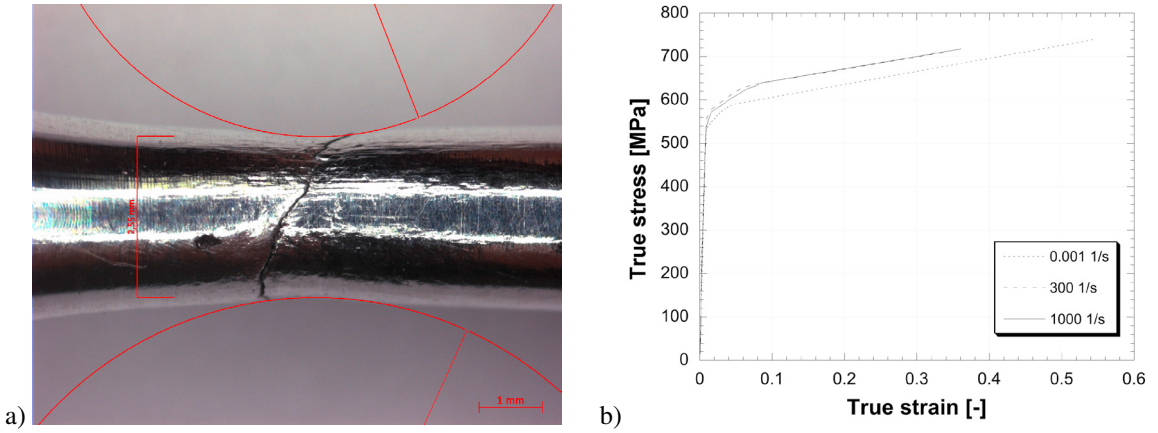


Fig. 7. (a) True stress versus true strain at different strain rates; (b) Photo of the specimen after a high strain rate test.

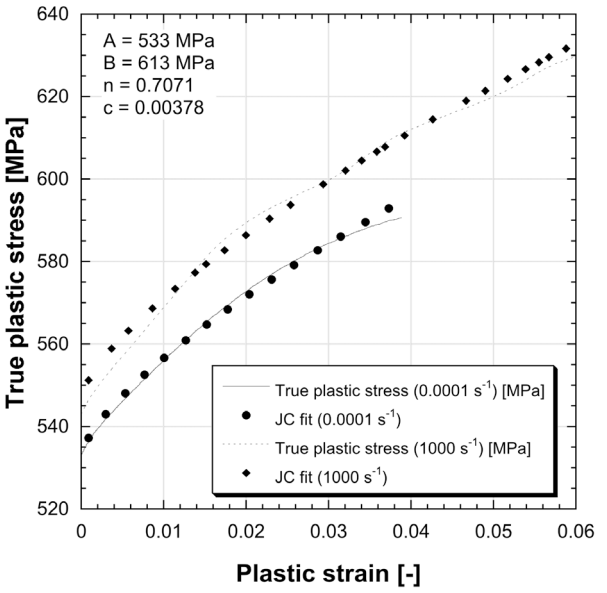


Fig. 8. Comparison between the experimental results and the predictions of Johnson?Cook material model for the true stress versus true plastic strain curves of AA7081 at different strain rates.

the experimental data. $A$ is the true yield stress of the material at the strain rate of $0.001 s^{-1}$. The material parameters $B$ and $n$ represent the strain hardening effects of the material at the strain rate $0.001 s^{-1}$. The strain rate sensitivity parameter is represented by the $C$ parameter. The temperature effects are not taken into account in this case. On substituting the Johnson-Cook model parameters in the eqn. (4), the concrete equation of this model is obtained for AA7081 as eqn. (5).

$$\sigma_{JC} = \left(533 + 613 \cdot \epsilon_p^{0.7071}\right) \cdot \left(1 + 0.0378 \cdot ln(\dot{\epsilon}^*)\right) \tag{5}$$

The comparisons between the predictions from Johnson-Cook model and experimental results at low and high strain rates are shown in Fig.8.

## 5. Conclusions

The dynamic tensile behavior of a commercial alluminium alloy AA7081 at different strain rates in the range 0.001-1000 $s^{-1}$ is presented. Mechanical properties in tension were determined using round samples, employing three different testing techniques: a universal electro-mechanic machine, a Hydro-Pneumatic machine and a Split Hopkinson Tensile Bar apparatus. The test results were used to obtain parameters for the Johnson-Cook constitutive law. The results highlighted a moderate strain rate sensitivity of the mechanical characteristics that can be considered in the design of lightweight defense vehicles.

## Acknowledgements

The Authors would like to acknowledge Aleris Aluminium Koblenz GmbH for providing the materials.

## References

Albertini, C., Montagnani, M., 1976. Wave propagation effects in dynamic loading. Nuclear Engineering and Design 37, 115 – 124.

Albertini, C., Montagnani, M., 1984. Testing techniques based on the SHPB, in: Inst of physics conf series, pp. 22–32.

Asprone, D., Cadoni, E., Prota, A., Manfredi, G., 2009. Strain-rate sensitivity of a pultruded e-glass/polyester composite. ASCE - Journal of Composites for Construction 13, 558–564.

Bridgman, P., 1952. Studies in large plastic flow and fracture. McGraw-Hill.

Cadoni, E., Dotta, M., Forni, D., Bianchi, S., Kaufmann, H., 2012a. Strain rate effects on mechanical properties in tension of aluminium alloys used in armour applications. EPJ Web of Conferences 26, 05004.

Cadoni, E., Dotta, M., Forni, D., Spaetig, P., 2011a. Strain-rate behavior in tension of the tempered martensitic reduced activation steel Eurofer97. Journal of Nuclear Materials 414, 360 – 366.

Cadoni, E., Dotta, M., Forni, D., Tesio, N., 2011b. Dynamic behaviour of reinforcing steel bars in tension. Applied Mechanics and Materials 82, 86–91.

Cadoni, E., Dotta, M., Forni, D., Tesio, N., 2014. High strain rate behaviour in tension of steel B500A reinforcing bar. Materials and Structures , 1–11.

Cadoni, E., Dotta, M., Forni, D., Tesio, N., Albertini, C., 2013. Mechanical behaviour of quenched and self-tempered reinforcing steel in tension under high strain rate. Materials and Design 49, 657 – 666.

Cadoni, E., Fenu, L., Forni, D., 2012b. Strain rate behaviour in tension of austenitic stainless steel used for reinforcing bars. Construction and Building Materials 35, 399 – 407.

Chen, Y., Clausen, A., Hopperstad, O., Langseth, M., 2009. Stressstrain behaviour of aluminium alloys at a wide range of strain rates. International Journal of Solids and Structures 46, 3825 – 3835.

Higashi, K., Mukai, T., Kaizu, K., Tsuchida, S., Tanimura, S., 1991. Strain rate dependence on mechanical properties in some commercial aluminum alloys. J. Phys. IV France 01, C3–341–C3–346.

Johnson, G., Cook, W., 1985. Fracture characteristics of three metals subjected to various strains, strain rates, temperatures and pressures. Engineering Fracture Mechanics 21, 31–48. Cited By 1512.

Oosterkamp, L.D., Ivankovic, A., Venizelos, G., 2000. High strain rate properties of selected aluminium alloys. Materials Science and Engineering: A 278, 225 – 235.

Peixinho, N., Doellinger, C., 2010. Characterization of dynamic material properties of light alloys for crashworthiness applications. Materials Research 13, 471 – 474.

Riganti, G., Cadoni, E., 2014. Numerical simulation of the high strain-rate behavior of quenched and self-tempered reinforcing steel in tension. Materials and Design 57, 156 – 167.

Singh, N., Singha, M., Cadoni, E., Gupta, N., 2012. Strain rate sensitivity of an aluminium alloy under compressive loads. Advanced Materials Research 548, 169–173.

Singh, N., Singha, M., Cadoni, E., Gupta, N., 2013. Dynamic characteristics of aluminium alloys at wide range of strain rates. Proc. Indian Natn.Sci. Acad. 79, 587–595.

Tanimura, S., Hayashi, H., Yamamoto, T., Mimura, K., 2009. Dynamic tensile properties of steels and aluminum alloys for a wide range of strain rates and strain. Journal of Solid Mechanics and Materials Engineering 3, 1263–1273.